DTU Library

Adaptive Trailing Edge Flaps for Load Reduction

Bergami, Leonardo

Publication date:
2011

Document Version
Publisher's PDF, also known as Version of record

[Link back to DTU Orbit](#)

Citation (APA):
Bergami, L. (2011). *Adaptive Trailing Edge Flaps for Load Reduction*. Paper presented at 7th PhD Seminar on Wind Energy in Europe, Delft, Netherlands.

Adaptive Trailing Edge Flaps for Active Load Reduction

Leonardo Bergami

Wind Energy Division, Ris DTU - National Laboratory for Sustainable Energy,
VEA-118, Frederiksborgvej 399, 4000 Roskilde, Denmark
E-mail: leob@risoe.dtu.dk

Keywords: smart rotors, ATEF, active load control

1 INTRODUCTION

The size of modern utility-scaled horizontal-axis wind turbines shows a continuously increasing trend. As the rotor size increases, the loads affecting the wind turbine scale up, not only as an effect of the increased mass of the structure, but also as a consequence of larger variations in the flow field spanned by the wind turbine blades; such variations originate, for instance, from atmospheric turbulence, wind shear, tower shadow, and wakes from other turbines.

Future generations of wind turbines would benefit from, and maybe necessitate, a control system able to alleviate the loads on the structure, for instance, by, for instance, actively controlling the aerodynamic forces along the blades so to compensate for variations in the flow field.

The concept is known as *smart rotor*: the active control system collects information on the current wind turbine state through different *sensors*, the informations are then processed by a *control algorithm*, and sent to *actuators* modifying the aerodynamic forces along the blade.

Several institutions in Europe and US are investigating smart rotor potentialities [1, 2], and different control strategies and actuator devices have been proposed. Some solutions point at using already existing actuators, as the pitch system, and integrate it with sensors and control algorithms so to control each blade pitch individually [3]. Other studies propose to use actuators that modify the aerodynamic forces locally along the blade span, as, for instance, micro-tabs[4], rotating flaps, or adaptive trailing edge flaps [5, 6].

The current work focuses on an adaptive trailing edge flap (ATEF) active control system, where the flap actuator deflects the aft part of the airfoil section by applying a smooth and continuous deformation shape to the airfoil camber line. Compared to a classic rotating flap, the continuous deformation shape results in better lift over drag performances, and lower noise emissions.

The paper briefly presents the aerodynamic model for lift, drag and moment on an airfoil undergoing arbitrary motion and flap deflection. In the following section, indications on the design process and requirements to the active flap control system are retrieved from a preliminary load analysis on the NREL 5-MW wind turbine in its baseline configuration [7]. Future work will then aim at designing an active flap control solution for the studied wind turbine, and assess the benefits of the active control system on the overall loading conditions.

2 MODEL AND METHOD

The presence of active flap devices poses new challenges in the modeling of the aerodynamic forces that generates along the wind turbine blades. CFD tools like Reynolds Averaged Navier Stokes (RANS) solvers provide accurate solutions, but the computation requirements are still too demanding for the tool to be efficiently integrated in an aeroelastic simulation tool.

Most simulation tools used to compute the aeroelastic response of a wind turbine in the time domain are based on implementations of the Blade Element Method (BEM) [8]. Under the BEM assumption of independent annular elements on the rotor plane, the rotor aerodynamic is determined from the lift and drag forces along the blades; the aerodynamic forces are then computed independently for each 2D airfoil section in which the blade has been discretized into.

This work presents an aerodynamic model to compute lift, drag, and moment coefficients for an airfoil section equipped with an Adaptive Trailing Edge Flap. The model reproduces both steady and dynamic characteristics of the forces on the airfoil undergoing arbitrary (within the limits of plane wake assumption) motion and flap deflection. The dynamic effects reproduced by the model can be split into three categories.

Added mass effects, or *non-circulatory* contributions, describe the forces that arise simply as a reaction of the fluid accelerated by the airfoil (or the flap) motion. The term has no memory effects, and only depends on the instantaneous motion of the airfoil or flap.

Effects from *wake dynamics*, or *potential flow* effects, describe the memory effects of the vorticity shed into the wake, following a change of the airfoil aerodynamic loading, as, for instance, due to a variation in angle of attack or flap deflection.

Dynamic stall effects represent the dynamics of the forces on an airfoil undergoing flow separation (stall).

2.1 Potential flow part

In this part of the model, the aerodynamic forces are computed assuming the airfoil always operates in fully attached flow conditions; viscous effects on the aerodynamic forces are thus neglected (potential flow assumption).

The deficiency, or time lag, on the lift force, caused by the vorticity shed into the wake, is modeled through an equivalent effective downwash speed, as in the model from Hansen et al. [9].

Gaunaa [10] shows that, under the assumptions of potential flow and thin-airfoil theory, the effective downwash speed for an airfoil undergoing arbitrary motion and camber line deformation can be evaluated as a superposition of indicial step responses. The indicial response function is expressed in an exponential form, similar to Jones's function for the flat plate response, thus allowing for an efficient time step integration algorithm.

The effective downwash speed is then split into an equivalent effective angle of attack α_{eff} and flap deflection β_{eff} contributions; the effective angle of attack and flap deflection are used in the look-up of the input steady data, returning thus aerodynamic forces that account for the wake memory effects.

2.2 Dynamic stall part

The flow separation part of the model follows the Beddoes-Leishmann dynamic stall formulation given in Hansen et al. [9]. The circulatory lift is expressed as a weighted sum of a fully attached and a fully separated contribution:

$$C_L^{\text{Circ.Dyn}} = C_L^{\text{att}} f^{dyn} + C_L^{\text{fs}}(1 - f^{dyn}). \qquad (1)$$

The dynamics of the flow separation along the airfoil are described through the separation function f^{dyn}, which assigns the weight between the fully attached and the fully separated component. The value of the function depends on the potential flow lift, and on a steady separation function f^{st}.

The steady values of the separation function f^{st}, fully attached C_L^{att}, and fully separated C_L^{fs} lift coefficients are retrieved from the steady input data C_L^{st}. All the quantities are now function of both angle of attack and flap deflection, and their computation is not as straightforward as in the rigid airfoil case. The computations are performed in an external 'preprocessing unit', which allows the user to check, and, eventually, correct the steady data that will be used as input in the aerodynamic model.

In the preprocessing unit, the steady state input lift C_L^{st} is split into a fully attached and a fully separated contribution, assuming that the fully attached part has a linear dependency on both angle of attack α and flap deflection β:

$$C_L^{lin} = \frac{\partial C_L}{\partial \alpha}(\alpha^{st} - \alpha_0) + \frac{\partial C_L}{\partial \beta}\beta^{st}. \qquad (2)$$

The steady separation function is then computed from the expression for the flat-plate lift in Kirchoff flow, as:

$$f(\alpha,\beta)^{\text{st}} = \left(2\sqrt{\frac{C_L^{st}}{C_L^{lin}}} - 1\right)^2. \qquad (3)$$

The separation function should be real and bounded $0 \leq f^{\text{st}} \leq 1$, thus singularities arise whenever $C_L^{st}/C_L^{lin} < 0$ or $C_L^{st}/C_L^{lin} > 1$. The singularities are avoided by simply rounding the function to the closest boundary value; further 'manual adjustments' will need to be applied by the user to avoid discontinuities in the lift coefficient and separation function input data.

Once the separation function f^{st} is determined, three flow regions are identified.

Fully attached region, where the separation function is $f^{st} = 1$. Here, C_L^{att} is taken equal to C_L^{st}, rather than C_L^{lin}, so to maintain the steady lift coefficient equal to the input one:

$$f^{st} = 1 \quad \rightarrow \quad \begin{cases} C_L^{att} = C_L^{st} \\ C_L^{fs} = C_L^{st}/2 \end{cases} ; \qquad (4)$$

Fully separated region, where the separation function is $f^{st} = 0$:

$$f^{st} = 0 \quad \rightarrow \quad \begin{cases} C_L^{fs} = C_L^{st} \\ C_L^{att} = C_L^{lin} \end{cases} ; \qquad (5)$$

Transition region:

$$0 < f^{st} < 1 \quad \rightarrow \quad \begin{cases} C_L^{att} = C_L^{lin} \\ C_L^{fs} = \frac{C_L^{st} - C_L^{lin} f^{st}}{1 - f^{st}} \end{cases} . \qquad (6)$$

The model has been validated by comparison with RANS solutions for an airfoil undergoing harmonic pitching motion and flap deflection, and it has been implemented in the multi-body aeroelastic simulation tool HAWC2 [11].

2.3 Method

The aeroelastic simulation tool HAWC2 is used to evaluate the aeroelastic response of the NREL 5-MW baseline wind turbine [7] in the time domain. A wide set of simulation conditions is outlined following the design load cases (DLC) prescribed by the IEC standard [12]; simulations include both stochastic, and deterministic wind fields inputs, normal operation and extreme events. The resulting simulated loads are summarized in terms of ultimate loads, and equivalent fatigue loads.

The equivalent fatigue loads are computed from the simulated time series by applying a Rain Flow Counting algorithm, and Palmgren-Miner rule for linear fatigue damage. The equivalent fatigue loads account for the amount of time the wind turbine is expected to spend in each simulated condition. A relative fatigue contribution k is evaluated as the ratio between the fatigue damage accumulated in a specific operation condition, and the total life-time fatigue damage.

3 PRELIMINARY LOAD ANALYSIS

A preliminary analysis is carried out on the NREL 5-MW baseline wind turbine. The analysis of the wind turbine in its baseline configuration allows to identify the DLC that are critical in terms of fatigue or ultimate loads. Active load alleviation in these specific cases would directly benefit the whole wind turbine structure. The critical cases provide thus a convenient set of simulation conditions for designing, testing, and assessing the performances of the active load control system.

Fatigue loads have been monitored at the blade root, in flapwise (M_x), edgewise (M_y), and torsion (M_z), at the tower base flange in fore-aft (M_{FA}) and side-to-side (M_{SS}) directions, and for the main shaft torsion (M_{DT}).

Relative contributions to the total life-time fatigue damage are grouped according to the operation condition that has generated the fatigue damage, figure 1. Operations in normal power production (DLC 1.1) are responsible for most of the fatigue loads on the structure, mainly because of the time the turbine is expected to spend in these conditions. Therefore, an active load alleviation system operating during normal power production can yield to a sensible reduction of the overall fatigue damage.
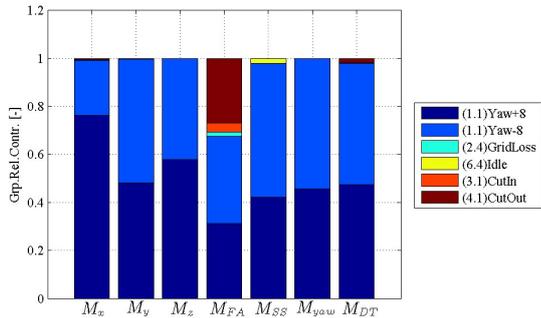
Figure 1: Fatigue damage relative contributions grouped by operation condition.

The same load-measuring locations are used to monitor ultimate loads; the maximum loads reported in each operation condition are plotted in figure 2. The highest simulated loads occur for operations under an extreme coherent gust (DLC 2.3), extreme turbulence (DLC 1.3), or extreme coherent gust with direction change (DLC 1.4). These cases should be thus considered during the design process of the active load control system, since a reduction of these maximum loads might yield a beneficial reduction of the overall structural requirements.

To obtain an overview on which frequency range the active control should focus on, an attempt is made to determine which frequencies returns the highest fatigue load contributions. A frequency spectrum is retrieved from the simulated loads, and Benasciutti and Tovo's [13] method is applied to
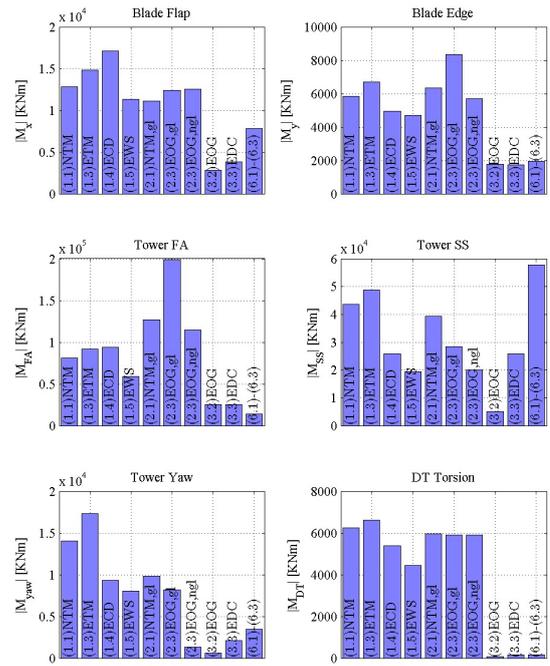
**Figure 2:** Ultimate load analysis. Maximum loads reported in each simulation condition.

obtain an equivalent fatigue damage rate from the load spectrum. The relative contribution from each frequency range is determined by setting to zero its spectral energy content and comparing the resulting fatigue damage rate with the original-full spectrum fatigue damage.

The result is presented as a 'fatigue-spectrogram' plot, figure 3, where the relative contributions to fatigue damage depend on both frequency and wind speed; red colors indicate higher fatigue contributions. The relative contributions from different wind speeds account for the time each wind speed bin is expected to occur.

For the blade flapwise root moment, figure 3, the largest fatigue contributions originate at high wind speeds, and from frequencies close to 1P (and its harmonics). Furthermore, both for blade and tower loads (not shown here), frequencies above 5 Hz yield only a modest contribution to the overall fatigue damage.

To conclude, the preliminary load analysis allows to identify a set of load cases which are critical in terms of either fatigue or ultimate loads. This reduced set of cases provides a convenient test field for the future design of the active control system, as load alleviation in these design cases would yield a direct benefit on the overall loading conditions.

Fatigue analysis in the frequency domain have highlighted that the highest contributions to the fatigue damage originates from loads with frequencies below 5 Hz, giving thus
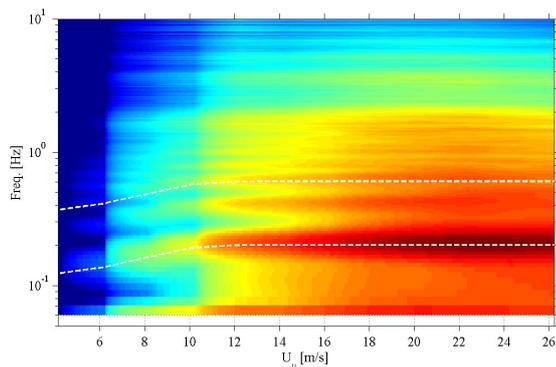
Figure 3: Fatigue analysis in the frequency domain. Blade flap-wise root moment, relative contribution to the total fatigue damage from different frequencies and wind speeds.

a clear indication on the frequency range the active control system should focus on.

4 FUTURE WORK: ACTIVE LOAD CONTROL

An active load control system will be designed for the NREL 5-MW reference wind turbine, using Adaptive Trailing Edge Flaps actuators, and structural loads sensors. First, the placement of the ATEF sections along the blade span needs to be optimized, accounting for factors as the flap effect on the measured loads, time delay, and structural constraints.

Once the flap positions have been fixed, the ATEF control algorithm is designed; the requirements outlined in the previous analysis, as well as the critical set of load cases will help in the design process. The control algorithm will most likely be a Model Predictive Control, and system identification techniques will be investigated in order to obtain the linear model required by the MPC controller.

The flap actuators and the active load control algorithm will be included in the aero-servo-elastic model of the NREL 5-MW wind turbine, and simulation will be performed with the HAWC2 code. As in the preliminary analysis, simulation conditions will be based on the design load cases prescribed in the IEC standard [12], and the loads will be evaluated in terms of equivalent fatigue loads and ultimate loads.

A comparison of the fatigue and ultimate loads resulting from simulations with and without active flap control will directly measure the impact of the ATEF system on the overall turbine loading conditions; as well as that, the comparison will bring new elements to be considered in the (ineluctably iterative...) design process. Finally, the comparison between flap and baseline configurations will allow to quantify the potential of the ATEF system for active load alleviation on MW-sized wind turbines.

REFERENCES

[1] T. K. Barlas and G. van Kuik. State of the art and prospectives of smart rotor control for wind turbines. *Journal of Physics: Conference Series*, 75(1):012080 (20 pp.), 2007. Journal Article.

[2] Matthew A. Lackner and Gijs van Kuik. A comparison of smart rotor control approaches using trailing edge flaps and individual pitch control. *Wind Energy*, 13(2-3):117–134, March 2010.

[3] T. J. Larsen, H. A. Madsen, and K. Thomsen. Active load reduction using individual pitch, based on local blade flow measurements. *Wind Energy*, 8(1):67–80, 2005. Journal Article.

[4] Scott J. Johnson, Jonathon P. Baker, C. P. van Dam, and Dale Berg. An overview of active load control techniques for wind turbines with an emphasis on microtabs. *Wind Energy*, 13(2-3):239–253, March 2010.

[5] Peter Bjoern Andersen, Lars Henriksen, Mac Gaunaa, Christian Bak, and Thomas Buhl. Deformable trailing edge flaps for modern megawatt wind turbine controllers using strain gauge sensors. *Wind Energy*, 13(2-3):193–206, March 2010.

[6] A. W Hulskamp, J. W van Wingerden, T. Barlas, H. Champliaud, G. A. M van Kuik, H. E. N Bersee, and M. Verhaegen. Design of a scaled wind turbine with a smart rotor for dynamic load control experiments. *Wind Energy*, 14(3):339–354, April 2011.

[7] J. Jonkman, S. Butterfield, W. Musial, and G. Scott. Definition of a 5-MW reference wind turbine for offshore system development. Technical Report NREL/TP-500-38060, National Renewable Energy Laboratory (NREL), February 2009.

[8] Martin Hansen. *Aerodynamics of wind turbines : rotors, loads and structure*. James & James, London, 2000.

[9] Morten Hartvig Hansen, Mac Gaunaa, and Helge Aagaard Madsen. A Beddoes-Leishman type dynamic stall model in state-space and indicial formulations. Technical Report R-1354(EN), Risoe National Laboratory, Roskilde (DK), 2004.

[10] M. Gaunaa. Unsteady two-dimensional potential-flow model for thin variable geometry airfoils. *Wind Energy*, 13(2-3):167–192, 2010.

[11] Torben Juul Larsen. How 2 HAWC2 the user's manual. Technical Report R-1597(EN), Risoe National Laboratory. Technical University of Denmark, 2009.

[12] International Electrotechnical Commission. IEC 61400-1: Wind turbines part 1: Design requirements. Technical report, International Electrotechnical Commission, 2005.

[13] D. Benasciutti and R. Tovo. Comparison of spectral methods for fatigue analysis of broad-band gaussian random processes. *Probabilistic Engineering Mechanics*, 21(4):287–299, October 2006.